



HAL
open science

Reliability and availability modelling of a retrofitted Diesel-based cogeneration system for heat and hot water demand of an isolated Antarctic base

Miguel Coronado, Benjamin Kadoch, Jorge Contreras, Fredy Kristjanpoller

► To cite this version:

Miguel Coronado, Benjamin Kadoch, Jorge Contreras, Fredy Kristjanpoller. Reliability and availability modelling of a retrofitted Diesel-based cogeneration system for heat and hot water demand of an isolated Antarctic base. *Eksploatacja i Niezawodność - Maintenance and Reliability*, 2023, 25 (3), 10.17531/ein/169779 . hal-04481992

HAL Id: hal-04481992

<https://hal.science/hal-04481992>

Submitted on 28 Feb 2024

HAL is a multi-disciplinary open access archive for the deposit and dissemination of scientific research documents, whether they are published or not. The documents may come from teaching and research institutions in France or abroad, or from public or private research centers.

L'archive ouverte pluridisciplinaire **HAL**, est destinée au dépôt et à la diffusion de documents scientifiques de niveau recherche, publiés ou non, émanant des établissements d'enseignement et de recherche français ou étrangers, des laboratoires publics ou privés.



Distributed under a Creative Commons Attribution 4.0 International License



Article citation info:

Coronado M, Kadoch B, Contreras J, Kristjanpoller F, Reliability and availability modelling of a retrofitted Diesel-based cogeneration system for heat and hot water demand of an isolated Antarctic base, *Eksploracja i Niezawodność – Maintenance and Reliability* 2023; 25(3) <http://doi.org/10.17531/ein/169779>

Reliability and availability modelling of a retrofitted Diesel-based cogeneration system for heat and hot water demand of an isolated Antarctic base

Indexed by:



Miguel Coronado^a, Benjamin Kadoch^b, Jorge Contreras^c, Fredy Kristjanpoller^{a,*}

^a Industrial Engineering Department, Universidad Técnica Federico Santa María, Chile

^b Aix Marseille Université, CNRS, IUSTI, Marseille, France

^c EPROIC Ingeniería y Construcción Ltda, Viña del Mar, Chile

Highlights

- The extreme conditions and fragile environment of Antarctica are considered.
- A continuous Markov Model is used to estimate the system reliability index.
- A waste heat recovery system in a diesel generator set is developed.
- The influence of hot water consumption profile and storage size is studied.
- The addition of a storage makes the system more efficient and more sustainable

Abstract

The reduction of greenhouse gas emissions is a relevant challenge for a sustainable development. Waste heat could be used to produce hot water by using a recovery system. This article studies the availability of a combined heat and power systems (CHP) in extreme area (Antarctic) through the integration of a waste heat recovery system with a diesel generator to produce hot water. The reliability and availability principles are incorporated to explore how the profile of hot water consumption and the hot water storage tank size affect system availability. Different combined heat and power systems are thus classified, and their availability indexes modelled by adopting the continuous Markov approach and the state space model. The results indicate that the CHP systems availability is strongly influenced by the daily hot water demand profile. As a useful recommendation, one of the considerations for increasing availability, reducing costs and greenhouse gas emissions with the CHP system is to include a hot water tank in the analysis.

Keywords

reliability, availability, waste heat recovery, combined heat and power

This is an open access article under the CC BY license (<https://creativecommons.org/licenses/by/4.0/>)

1. Introduction

Although fossil fuels will remain the primary source of energy for drinking water, heating, lighting, and electricity in Antarctica for years to come, it is necessary to look for new ways to reduce our dependence on them. Due to their versatility to produce electricity, diesel generators are widely used in rural and isolated locations, such as Antarctic bases. However, several losses are produced by the engine exhaust gases, the cooling system and the heat conducted through the engine from combustion chamber to the surrounding environment [15]. Conklin and Szybist [7] reported that only 10.4% of fuel

consumed is converted into useful work.

Recovering part of the wasted heat to produce heat for industrial or domestic applications could increase efficiency up to 80% [16]. The generation of two different forms of useful energy, typically mechanical and thermal energy, from a single primary energy source is called cogeneration [9].

The interest of retrofitted engine-based cogeneration systems has been demonstrated to develop small cogeneration system in previous research works. For example, the performance of an internal combustion engine-based

(*) Corresponding author.

E-mail addresses:

M. Coronado (ORCID: 0009-0007-0630-5998) miguel.coronado.13@sansano.usm.cl, B. Kadoch (ORCID: 0000-0001-9346-1399) benjamin.kadoch@univ-amu.fr, J. Contreras (ORCID: 0000-0003-3277-7319) jorge.contrerasr@gmail.com, F. Kristjanpoller (ORCID: 0000-0001-8970-9371) fredy.kristjanpoller@usm.cl

cogeneration system for residential application was assessed by [2, 3]. They used primary energy, electricity consumption, associated greenhouse gas emissions and tolerable capital cost as indicators to evaluate cogeneration system architecture with thermal storage in "typical" single-storey houses located in five cities representing the main climatic regions of Canada.

The exhaust gas is used to produce hot water in a heat exchanger or heat recovery system. In case of failure of the generator, the whole cogeneration system is fully shut down since the hot water generation performance is dependent on the generator set availability. A reduction in availability can be caused by unplanned maintenance actions. In particular, the global performance of energy recovery systems for Diesel engines has been studied from a technical and economic perspective [6, 24, 27]. A recent critical review of the performance studies of waste heat recovery can be found in [10]. However, to the best of our knowledge, there are no studies evaluating the effects of different components on the availability of these systems. The calculation of the availability of a cogeneration system indicates the probability of operating in a specific period, where a satisfactory operation corresponds to the generation of electricity and heat during this defined period. The availability estimation is mainly based on the system reliability modelling, that indicates the probability that the system will perform its function adequately for a given period or that it will operate in a defined environment without failure. The mix of reliability and availability analysis plays a fundamental role in technical and economic feasibility studies by providing the operating time service of the system, which impacts the operational costs and the optimal maintenance schedule of these systems. Therefore, the performance of cogeneration system should consider availability to optimally estimate the electrical and thermal size of a particular installation. Due to complicated physical interactions between different subsystems that form a cogeneration system, reliability of whole system should be addresses in a modular and integrated approach, allowing the system availability estimation to develop the assessment of cogeneration systems [25].

In terms of reliability, Haghifam and Manbachi [14] classified the different subsystems of a cogeneration system and modeled their reliability, availability, and mean time failure indices as a function of the interactions between generation site

and consumption demand [30]. These authors used a state space model and a continuous Markov model but did not analyze the behavior during an evaluation period or based on a given demand; therefore, the cogeneration system could not be evaluated from a technical and economic point of view. Jiang et al. [17] used a combined cooling, heating and power (CCHP) system to evaluate the reliability of different components, highlighting their maintenance time and then assessing the maintenance cost. They also used the Markov model but did not evaluate the availability of the demand supply system and how it evolved in a specific period of time. The redundancy has been analyzed by same authors showing that this strategy can reduce total cost and improve the availability of a CCHP [18].

Some authors have carried out a sensitivity analysis for shell and tube heat exchangers [4, 23], for which they designed the devices for heat recovery, but did not evaluate the performance of these devices with exhaust gases and the availability that could be generated with them.

Reliability theory and applications have a great impact on the decision-making process in different fields. In the energy field, the analysis of operational reliability and maintainability is important when evaluating the availability of operative plant conditions [12, 21]. Reliability theory, from a life cycle perspective, offers important support for studying and generating proposals for the improvement of industrial plants [29]. Specifically, with respect to energy equipment and relevant processes, opportunities related to the design are a relevant success factor [11], and reliability assessment is crucial in performance evaluation as it involves technical and cost parameters [19]. Some experiences and methodologies for evaluating the reliability of power systems, especially for renewable energy sources (RES), are presented in [13].

The originality of the paper is to integrate the concept of reliability and availability for the dynamic study of thermal systems for heating and domestic hot water needs in a fragile and isolated environment. The goal is to study the influence of storage sizes and domestic hot water profiles on the dynamic and global availability of energy systems in order to propose efficient, reliable, cost-effective and low-emission solutions.

The analysis of availability with a dynamic approach, considers the modeling of a system with the aim of including all possible scenarios and thus incorporate realism and randomness

in the modeled production processes. This analysis helps to solve the trade-off of working with expected indicators of availability. Its great utility has been demonstrated in shared loading systems, transport and distribution systems [22].

The remainder of the manuscript describes the methodology used for reliability, availability, and energy modelling in Sect. 2. Sect. 3 details the Chilean Antarctic base case study and the corresponding results are shown and discussed in Sect. 4. Finally, some conclusions are given in Sect. 5.

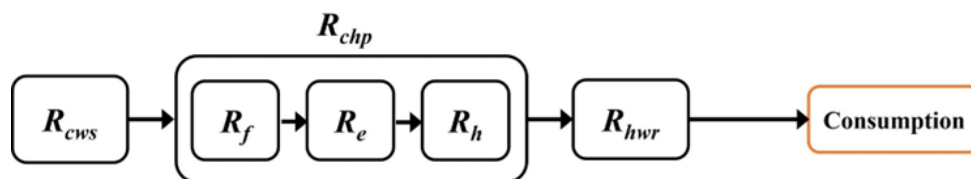


Figure 1. Simple model of the system to evaluate reliability of the cogeneration system to the final consumption point.

2.1. Cogeneration system reliability modelling

The cogeneration system is split into three subsystems that are considered independently in the simulation process. Based on this model, a scheme of the reliability network of the cogeneration system to the consumption point is shown in **Błąd! Nie można odnaleźć źródła odwołania.** The three subsystems are in series: the cold-water supply network (R_{cws}), the cogeneration system itself (R_{CHP}) and the hot water reservoir (R_{hwr}). Mathematically, the reliability of the system is described by equation (eq.1):

$$R_s = R_{cws} \cdot R_{CHP} \cdot R_{hwr} \quad (1)$$

The concept of reliability requires incorporating failure probabilities and associated costs that depend on failure rates, operation hours, number of equipment considered with or without redundancy and failure conditions of the power sources. Two important parameters are used for reliability modelling: failure rate (λ), which determines the number of failures in a specific period of time, and repair rate (μ), which determines the frequency of repair in that period. The reliability of each sub-system can be calculated as $R = \mu / (\lambda + \mu)$.

In this way, the reliability of the cogeneration system (R_{CHP}) is modelled by the individual reliability of three subsystems, that are also related in a serial configuration. These three reliabilities concern the fuel supply system (R_f), the electricity generation (R_e) and the heat recovery system (R_h). The reliability of the cogeneration system is then expressed as:

2. Methodology

For the reliability modelling of combined heat and power systems, electricity-generation, fuel-delivery, and heat-generation subsystems, as well as the water-delivery network to the CHP and the hot-water-delivery network to the consumer, constitute the set of subsystems considered.

$$R_{CHP} = R_f \cdot R_e \cdot R_h = \frac{\mu_e \cdot \mu_f \cdot \mu_h}{(\lambda_e + \mu_e)(\lambda_f + \mu_f)(\lambda_h + \mu_h)} \quad (2)$$

This relationship represents the reliability of the cogeneration system when all three subsystems work correctly but does not consider all the different operational states that may exist. For example, sometimes the electrical generation subsystem may not work properly, but the heat recovery subsystem does work and can recover the waste heat produced by the generator set. On the other hand, the heat recovery subsystem could fail but the electricity generation subsystem can work properly. The availability evaluates the reliability of a cogeneration system that has multiple states. This index allows to include all possible states in a cogeneration system model. Therefore, in the next sections, a procedure to estimate the availability index is described.

2.1.1. Cogeneration system availability modeling

The availability index represents the probability that the system is in each operating state of the cogeneration system. To calculate this index, the Markov Continuous Model based on the State Space Model is used considering the conditional probabilities of failure, repair, and preventive maintenance [14]. Markov-approach modeling can be used for continuous and discrete systems when a system is stationary with identifiable states and a lack of memory [5]. In a continuous Markov process [26], the probability of repairable system failure remains

constant in given time intervals. To demonstrate the continuous Markov concepts, a state space diagram is applied to represent system state changes. The operational probability of a single-component system is equal to the sum of the probability of being operative at time t and not failing at time $\delta t + t$, and of the probability of failure at time t and being repaired at time δt .

A continuous Markov process is a stochastic process, that takes values from the state space and satisfies the Markov property, to determine the probabilities of each system state. This stochastic process has the Markov property that the conditional probability distribution of future states of the process depends only on the current state. For better understanding of system behavior, it is recommended to determine indices such as availability and mean time to failure. Availability is related to the frequency of non-failure states. Based on the state space diagram, a frequency-balance technique is used with the continuous Markov approach to obtain reliability indices [5].

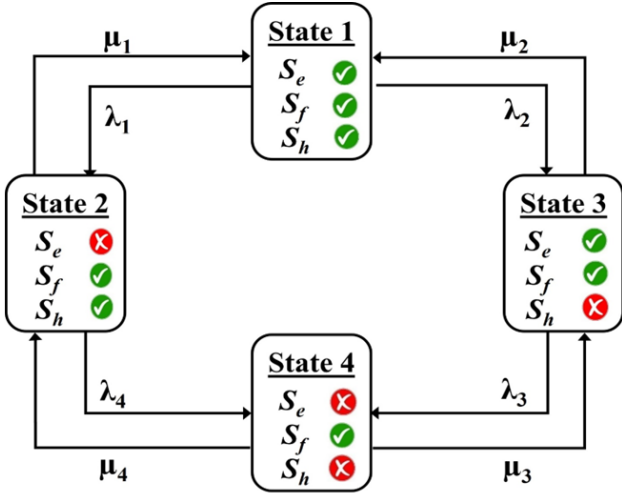


Figure 2. State space diagram of the cogeneration system.

Subscripts e, f and h correspond to fuel supply, electricity generation and heat recovery subsystems, respectively. λ and μ are related to failure and repair rates.

Figure 2 shows four states for the cogeneration system, based on the method used in [14]. When operating with the three subsystems, fuel supply (S_f), electricity generation (S_e) and heat recovery (S_h), eight possible states can be considered, but four of these are not useful for the required operational conditions, so only four possible states are considered for this analysis.

Based on this reasoning, in the cogeneration system model shown in Figure 2, the failure rates are expressed as: λ_1 when the whole subsystem works and the fuel supply subsystem fails,

λ_2 when the whole subsystem works and the heat recovery subsystem fails, λ_3 when the electricity generation subsystem fails after the heat recovery subsystem has failed, and finally, λ_4 when the heat recovery subsystem fails after the power supply subsystem has failed. Similarly, repair rates are expressed as: μ_1 when the fuel supply subsystem is repaired and the whole subsystem works, μ_2 when the heat recovery subsystem is repaired and the whole subsystem works, μ_3 when the electricity generation subsystem is repaired but the heat recovery subsystem still fails, and finally, μ_4 when the heat recovery subsystem is repaired but the power supply subsystem still fails.

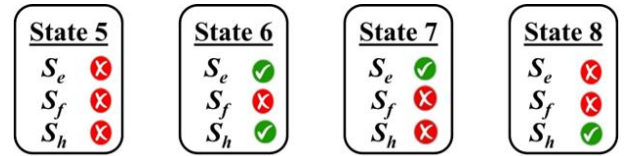


Figure 3. Irrelevant states.

On the other hand, when there is a failure in the S_f , the other two subsystems (S_h and S_e) fail since they require the fuel to operate. Therefore, the four states, shown in Figure 3, are not relevant in the Markov Process. Indeed, they are unavailable states in practice, which occurs when S_f fails and therefore all subsystems fail.

Heat recovery availability (A_h) is determined by the probability that the whole cogeneration system reaches state 1 and state 2. This can be obtained by using equation (eq.3). Moreover, the availability (A_h) of electricity generation subsystem is composed of probabilities for states 1 and 3, as can be seen in equation (eq.4).

$$A_h = P_1 + P_2 \quad (3)$$

$$A_e = P_1 + P_3 \quad (4)$$

Two methods are used to obtain the probabilities of states 1, 2 and 3: *the frequency balance approach* and *the stochastic transitional probability matrix* [5].

In the frequency balance approach, the expected frequency of a system entering a state must be equal to the expected frequency of exit from that state. The probabilities of each state are determined by solving the frequency balance equation system (equations (eq.5) to (eq.8)) and then applying equation (eq.9).

$$P_1 \cdot (\lambda_1 + \lambda_2) = P_2 \cdot \mu_1 + P_3 \cdot \mu_2 \quad (5)$$

$$P_2 \cdot (\mu_1 + \lambda_4) = P_1 \cdot \lambda_1 + P_4 \cdot \mu_4 \quad (6)$$

$$P_3 \cdot (\mu_2 + \lambda_3) = P_1 \cdot \lambda_2 + P_4 \cdot \mu_3 \quad (7)$$

$$P_4 \cdot (\mu_3 + \mu_4) = P_1 \cdot \lambda_8 + P_3 \cdot \lambda_3 + P_2 \cdot \lambda_4 \quad (8)$$

$$P_1 + P_2 + P_3 + P_4 = 1 \quad (9)$$

By obtaining the reliability of the cogeneration system (R_{CHP}), and assuming that the reliabilities of cold water supply network (R_{cws}) and hot water reservoir (R_{hwr}) tend to 100%, the total reliability of the system (R_s) is equal to R_{CHP} (see equation (eq.1)).

2.1.2. Energy model

An energy model is used to estimate available thermal energy from exhaust gases of the Diesel generator set. The available heat is a function of electricity demand which controls the load factor of generator and the fuel consumed. The availability factor is considered 1 with a probability of P_1 and 0 with a probability of $1 - P_1$. Although in an annual horizon the expected availability respects this value, it is possible that at specific intervals the availability is equal to 100% and at others that the system is completely unavailable due to maintenance activities. For this reason, availability is modeled with a random variable over the analysis period, considering that its average is the expected value. The fuel mass flow (\dot{m}_f) is calculated from the operational data of the generators in equation (eq.10):

$$\dot{m}_f = \frac{(\alpha \cdot de + \beta) \cdot \rho_f}{3600} \quad (10)$$

where α and β correspond to correlation parameters that allow to determine the volumetric flow of diesel fuel in L/h based on electricity demand (de), and the fuel density of fuel (ρ_f).

Subsequently, the energy rate supplied by fuel (\dot{E}_f), which depends on the electricity demand, is obtained according to equation (eq.11):

$$\dot{E}_f = \dot{m}_f LHV \quad (11)$$

where LHV is the lower heating value of fuel. The energy rate loss from engine through exhaust gases (\dot{Q}) is a fraction of the energy rate of fuel $\dot{Q}_{exh} = \dot{E}_f \cdot \phi$, where ϕ is the fraction of energy lost through exhaust gases. Equation (eq.12) gives the energy that should be recovered to increase water temperature when it flows through recovery system.

$$\dot{Q}_r = \dot{m}_w c_{p,w} (T_o - T_i) \quad (12)$$

The useful energy recovered from exhausts gases depends on the efficiency of the recovery systems (η_r) according to $\dot{Q}_r = \dot{Q}_{exh} \cdot \eta_r$. The total amount of water that the heat recovery subsystem can supply at a specific time is estimated with equation (eq.13):

$$\dot{m}_w = \frac{\dot{Q}_r}{(T_o - T_i) \cdot c_{p,w}} \quad (13)$$

This procedure is performed for each hour to account for the effect of the different hourly hot water consumption profiles on hot water availability. If the hot water supply to the system is not sufficient to meet the hot water demand in that period and the system does not have a hot water reservoir, it is considered as not available. If the system has a hot water reservoir, the latter acts as a buffer [25]. It is therefore responsible for accumulating the water that has not been used for a certain period of time or for supplying water when the heat recovery subsystem cannot provide all or part of it. The system availability and unavailability are calculated based on the hours during which the hot water service is not available, or the hot water demand is not met. This indicator is evaluated hour by hour considering the respective period duration.

To evaluate the environmental impact of the present system, the reduction of CO₂ emissions is also performed by considering the displacement of the oil consumed by the current boiler. It is calculated by using the recovered heat to meet the hourly hot water demand for each profile.

The innovation of this article is the application of the proposed methodology to a Chilean Antarctic base study case using Monte Carlo simulations, to evaluate the availability by different daily hot water demand profiles and incorporate a hot water tank in the analysis. As a main principle this methodology considers the integration of a waste heat recovery system with a diesel generator to produce hot water. The availability indexes modelled by adopting the continuous Markov approach and the state space model.

3. The case study: Chilean Antarctic base

In order to demonstrate the feasibility assessment methodology previously described operational Diesel fuel consumption data of the Base Presidente Eduardo Frei Montalva [8] is considered. This Diesel fuel is used to provide electricity and thermal energy consumed for heating and domestic hot water (DHW) demand. Currently, electricity and heating needs are covered by a Diesel generation set and a conventional Diesel boiler, respectively. The proposed configuration includes a 600 kVA diesel generator set with an exhaust heat recovery system for the cogeneration system. The heat recovery system generates hot water that is supplied to the consumption side by a hot-water-delivery

network. This arrangement is composed of four subsystems: the diesel generator set, the exhaust heat recovery system, the cold-water supply system, and the fuel supply system, necessary to operate the electric generator. The cogeneration system is integrated with an auxiliary system consisting of a hot water reservoir and a diesel boiler that supply the needs for hot water when the cogeneration system is not available or does not fully meet hot water demand. Figure 4, shows a representative diagram of the complete system from the generation site to the end user with the failure rates used.

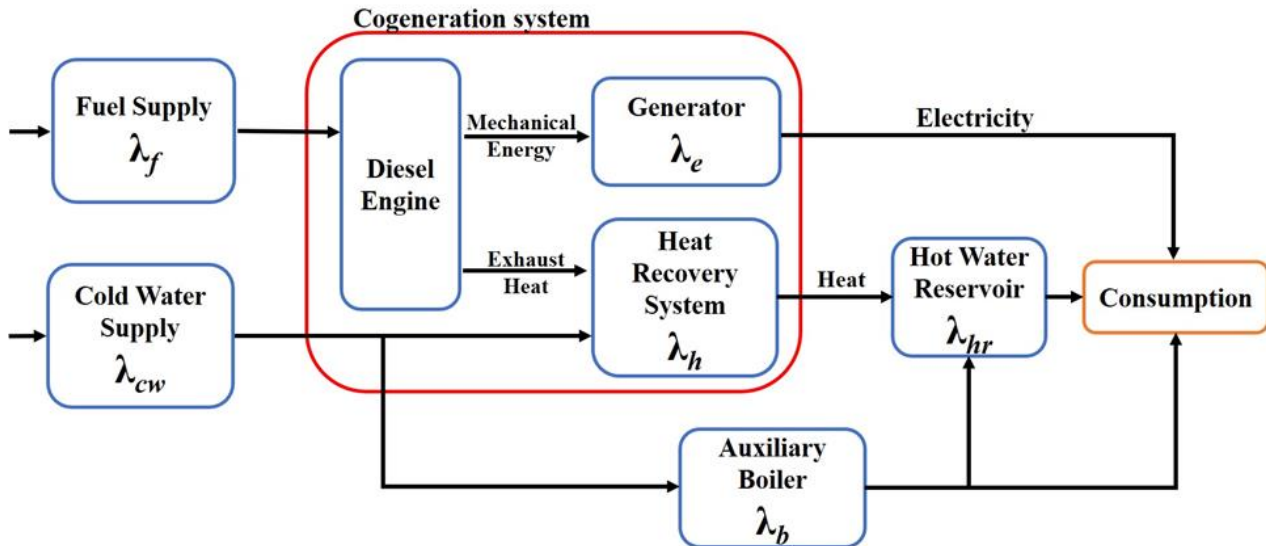


Figure 4. Cogeneration system from the generation site to the end user.

The diesel generator set used to simulate the performance of the proposed system is a Caterpillar brand, with a nominal power of 600 kVA working in a continuous rating all year long.

The electrical and thermal efficiencies are considered as constants in this study. To evaluate the effect of the size of the hot water reservoir, three different sizes are studied and compared with the performance of the system without a reservoir.

The auxiliary system is composed of a hot water reservoir and a boiler. As we are also interested in the effect of reservoir size on the level of availability of the whole system, the impact of the reservoir on the supply to the final consumer is analyzed, by evaluating the final availability of the system with and without a reservoir. The capacity and the cost of each reservoir are detailed in Table 1.

Table 1. Capacity and cost of hot water reservoirs.

Features	reservoir 1	reservoir 2	reservoir 3	reservoir 4	reservoir 5
Capacity (L)	1000	2000	3000	4000	5000
Cost (USD)	1930.72	4082.67	5991.03	7655.79	9076.95

Furthermore, for a more detailed analysis, a boiler, that supplies the demand for hot water when the cogeneration system is not available or does not fully satisfy the demand, is

considered. In this case, the auxiliary boiler operates with the performance parameters indicated in Table 2.

Table 2. Boiler parameters.

Boiler parameters		
η_b	60	(%)
LHV	43	(MJ)
ρ_f	0.832	(kg/L)
Diesel oil cost	1.807	(USD/L)

The demand is obtained from the fuel consumption of the boiler and the diesel power generator during in Antarctica, as shown in Figure 5.

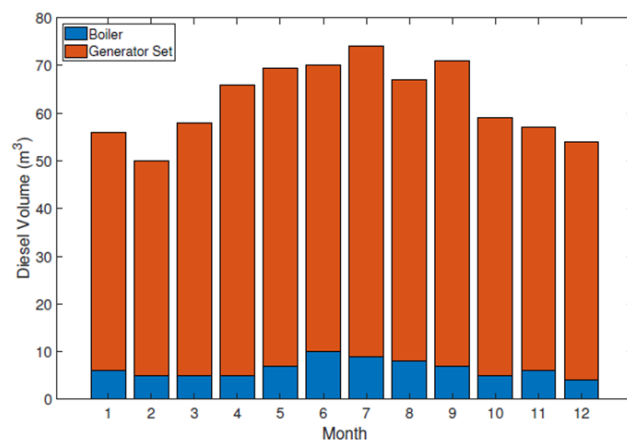


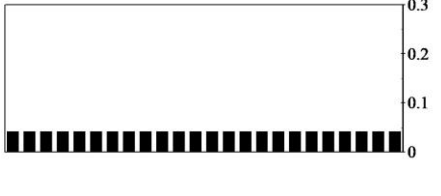
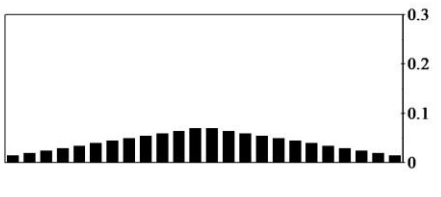
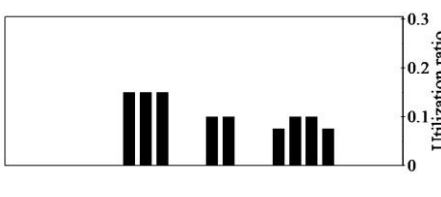

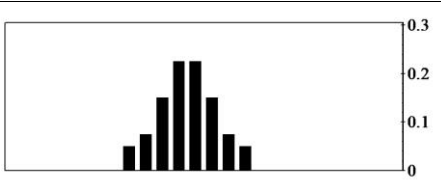
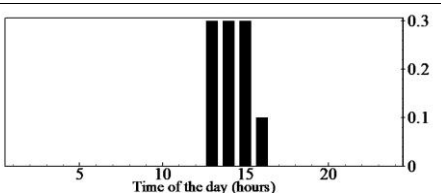
Figure 5. Diesel volume consumed by the Chilean Antarctic base along the year.

3.1. Hot water consumption

Hot water consumption in the Chilean Antarctic base is mainly for heating and domestic hot water. Six different profiles of

daily hot water consumption are considered to analyze the availability of the waste heat recovery system, which are described in **Błąd! Nie można odnaleźć źródła odwołania..**

Table 3. Profiles of hot water consumption [1]. Profiles are depicted as a fraction of the total amount along the day.

Profile description	Profile
<p>Profile 1: Uniform consumption over the day.</p>	
<p>Profile 2: Consumption gradually increases until peak hours and then decreases (cascade consumption).</p>	
<p>Profile 3: Based on domestic hot water consumption according to ISO 9459-3: 1007 [28].</p>	
<p>Profile 4: Uniform consumption between 8 and 16 h.</p>	
<p>Profile 5: Cascade consumption from 7 to 15 h</p>	
<p>Profile 6: Concentrated profile with 90% of consumption uniformly distributed between 13 and 15 h, 10% consumption at 16 h.</p>	

3.2. Calculation of system availability

The availability of the cogeneration system, consisting of the generator set and the waste heat recovery system, is calculated using the state space model and the continuous Markov model. Then, based on this availability, the Monte Carlo simulation is

used to calculate the total availability of the system for one year of operation, considering 8,760 hours per year.

3.2.1. State space and continuous Markov models

The reliability calculation with its parameters and considerations is presented below, using the state space and the

continuous Markov model. Table 4 shows the failure rates (λ) and repair rates (μ) of the system according to the state space presented in Figure 2. Based on the study conducted by Haghifam and Manbachi [14], the failure density function is described with an exponential distribution, and therefore the elements have a constant failure rate. This method provides an initial estimation, which is why a constant failure rate and exponential distribution are used. Haghifam and Manbachi [14], provides references for the failure rates and repair rates by besides the continuous Markov Approach and the state space model. To use this approach, an essential condition that should be satisfied is the Markov property. This property states that the future behavior of a stochastic process depends solely on its current state and is independent of its past states, given the present state [20].

Considering that failure density function and the repair time density function are described with an exponential distribution, is possible to confirm that Failure rate λ and Repair rate μ meet the conditions required for continuous Markov model. The Markov property in an exponential distribution can be demonstrated through the memoryless property of said distribution. The memoryless property states that the probability of an event occurring in the future does not depend on how much time has passed since a previous event occurred. To establish the Markov property in an exponential distribution, let us consider three points in time: t_1 , t_2 , and t_3 , where $t_1 < t_2 < t_3$. Our aim is to demonstrate that the exponential distribution between t_2 and t_3 depends solely on the difference between t_2 and t_3 , irrespective of what occurred before t_2 .

The exponential distribution with a rate parameter λ is defined as $f(x) = \lambda * e^{(-\lambda x)}$, for $x \geq 0$.

The probability of the event occurring at t_3 given that it did not occur at t_1 and t_2 can be computed using the probability density function (pdf) of the exponential distribution. Let us denote this probability as $P(X > t_3 | X > t_2, X > t_1)$, where X is a random variable with an exponential distribution.

We can employ the memoryless property to simplify this probability. The memoryless property states that:

$P(X > t_3 | X > t_2) = P(X > t_3 - t_2)$. In other words, the probability of the event occurring after t_3 , given that it did not occur before t_2 , is equal to the probability of the event occurring after a time interval equal to $(t_3 - t_2)$.

By repeatedly applying this property, we can simplify the desired probability as follows:

$$P(X > t_3 | X > t_2, X > t_1) = P(X > t_3 - t_2 | X > t_2, X > t_1) = P(X > t_3 - t_2 | X > t_2) = P(X > t_3 - t_2) = e^{(-\lambda(t_3 - t_2))}$$

Therefore, the probability of the event occurring at t_3 given that it did not occur at t_1 and t_2 is simply $e^{(-\lambda(t_3 - t_2))}$, which solely depends on the difference between t_2 and t_3 . This demonstrates that the exponential distribution possesses the Markov property, where the probability of a future event solely depends on the time elapsed since the last event.

Table 4. Failure rates (λ) and repair rates (μ) calculated with the Markov state space approach.

Failure rate	Value (f/Year)	Repair rate	Value (f/Year)
λ_1	2	μ_1	48
λ_2	0.3	μ_2	40
λ_3	0.1	μ_3	14
λ_4	0.4	μ_4	80

The probability of each state previously analyzed in the cogeneration system is shown in Table 5.

The availability of state 1, corresponding to the time when all the components of the cogeneration system are in operation, is $P_1 = 95.3\%$ according to the state space and continuous Markov model.

Table 5. Probability for each state in the cogeneration system.

State	Probability
P_1	0.9530
P_2	0.0397
P_3	0.0072
P_4	0.0001

According to these data and through the continuous Markov model, an availability of 0.9602 is obtained with equation (eq.14) for the electricity generation subsystem, which implies that 96.02% of the cases the system is available to generate electricity. On the other hand, the availability of the heat recovery system, obtained with equation (eq.15), corresponds to 0.9927, which implies that 99.27% of the cases the system is available to recover waste heat from the exhaust gases.

$$A_e = P_1 + P_3 = 0.9602 \quad (14)$$

$$A_r = P_1 + P_2 = 0.9927 \quad (15)$$

95.3% availability is used to calculate the total availability of the cogeneration system in a year that considers 8,760 hours. Indeed, the system must be in state 1 to be able to optimally meet the electrical and heat energy requirements.

3.2.2. Monte Carlo simulation

Based on the availability calculated using the *state space* and the *continuous Markov model*, Monte Carlo simulations are performed with the parameters of Table 6.

Table 6. Parameters used in the Monte Carlo simulation.

Parameters	Value	Unit
t	8,760	h
N	10,000	iteration
ρ_f	0.832	kg/L
ρ_w	0.997	kg/L
LHV	43	MJ/kg
ϕ	36.628	%
T_i	277.15	K
T_o	333.15	K
$c_{p,w}$	4.189	kJ/kg·K
η_r	25	%

Electricity demand is estimated based on the historical diesel consumption of the electric generator. The hourly consumption demand is obtained considering the volume of diesel historically consumed (Figure 5) and the previously generated demand profiles (**Błąd! Nie można odnaleźć źródła odwołania.**). In addition, a uniform distribution for electricity demand and a triangular distribution for thermal demand is considered.

3.2.3. Costs of the heat recovery system

The base cost is estimated as the cost of Diesel oil consumed based on the boiler's oil demand, projected over one year:

$$AC = P_{diesel} \cdot \sum_{i=1}^N V_{diesel} \quad (16)$$

where AC is the annual operational cost of the cogeneration system, V_{diesel} the daily volume of diesel consumed and P_{diesel} the price of Diesel in the Antarctic base. N is the number of operating hours in one year (8,760). The values of these parameters are displayed in Table 7. Based on operational data, the value of diesel currently consumed by the boiler is 77,000 L Table 7. Parameters to compute operational cost of reference case.

Parameters	Value	Unit
Diesel oil cost	1.807	USD/L
Boiler oil quantity	77,000	L
Heat recovery system	30,000	USD
Installation	5,000	USD

The investment cost of the heat recovery system is

considered as 30,000 USD for the construction of heat recovery system and 1,000 USD per day for a 5-day installation period. It should be noted that the cost of installing the waste heat recovery system without a heat reservoir is 35,000 USD.

3.2.4. Environmental impacts

To evaluate the environmental impact of implementing a heat recovering system, the reduction of CO_2 emissions is also considered. This reduction is generated by the displacement of the oil consumed by the current boiler. It is calculated by using the heat recovered to meet the hourly hot water demand according to each profile. This task is carried out by considering an emission factor of $0.27 \text{ kg } CO_2/kWh$

4. Results and discussion

Thirty-Six operational configurations are studied using the six hourly hot water consumption profiles and six hot water storage sizes. These configurations are used to evaluate the performance in terms of availability, operational cost and CO_2 emissions of the retrofitted cogeneration system.

4.1. Instant availability

Figure 6 illustrates the effect of the hot water storage size on the evolution of the instantaneous cogeneration system availability over a year, for each hot water consumption profile, as proposed in [1].

Instant availability evolution of the cogeneration system over a year, for the six hourly hot water consumption profiles and the six hot water storage sizes. Lines represent the availability for different water storage configurations (y_1 -axis) and shadowed bars represent the monthly hot water consumption (y_2 -axis).

In Figure 6a, the evolution of the instantaneous availability is exhibited when the hourly hot water consumption profile 1 is considered. In this configuration, except for the case with no hot water storage (black solid line) and for a 1000 L storage, the retrofitted cogeneration system availability is maximum up to day 150 for all sizes of reservoir. After day 150, the availability decreases because of a large increase in the monthly hot water consumption due to the winter season. The slope of the decrease is more pronounced in the system with no hot water storage (solid line). It is important to remark that the size of the hot water storage has a small effect on the evolution of the

availability. A difference can be observed by increasing the size from 1000 to 2000 L, but beyond 2000 L the improvement in

availability is negligible regardless of the size of the storage.

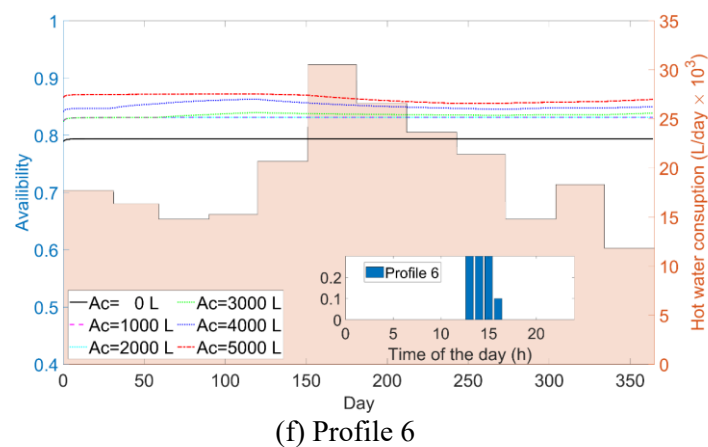
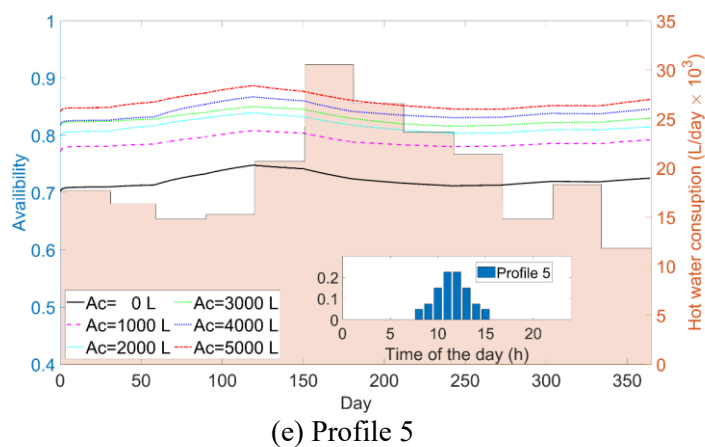
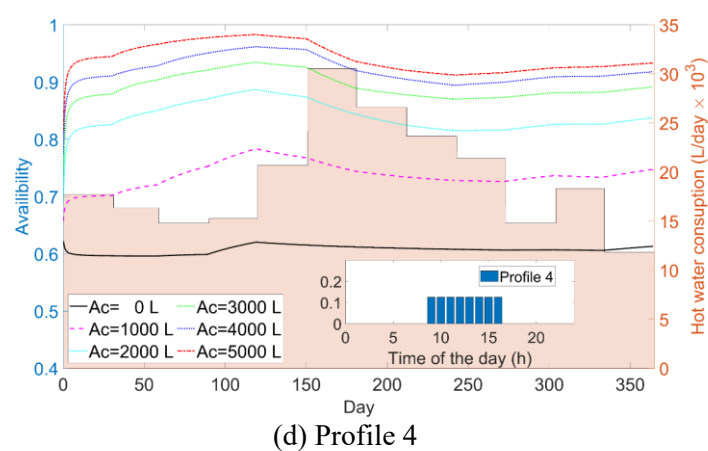
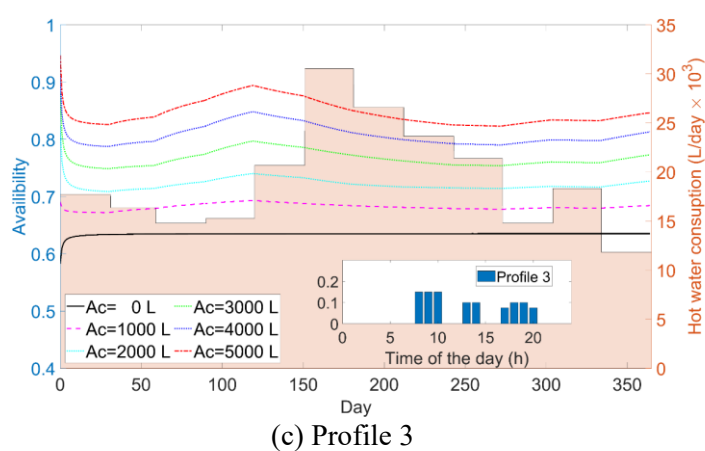
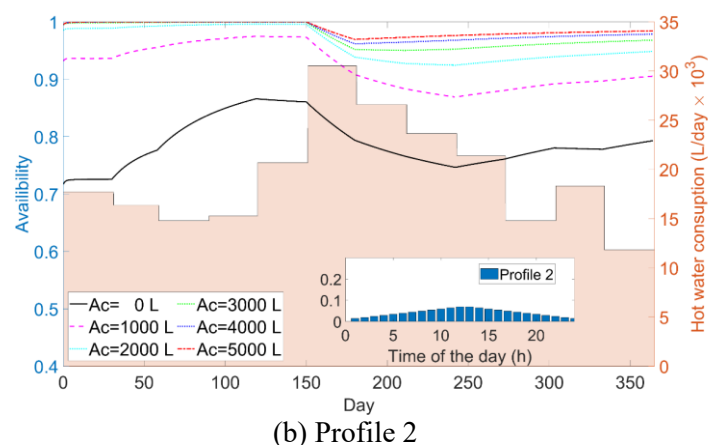
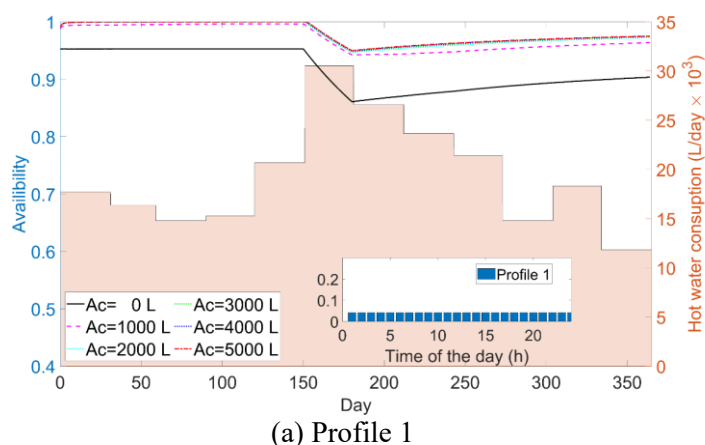


Figure 6. Instant availability evolution of the cogeneration system over a year, for the six hourly hot water consumption profiles and the six hot water storage sizes. Lines represent the availability for different water storage configurations (y_1 -axis) and shadowed bars represent the monthly hot water consumption (y_2 -axis).

Minimum availability is reached on day 180 for all cases. It can be noted that the effect of incorporating a hot water storage is most important that the size of the storage volume for this uniform hot water consumption profile. For example, when no hot water storage is considered, the minimum instant availability reached is 0.85 (day 181), while the minimum reached with hot water storage is 0.93 and 0.94 for volumes of

1000 and 5000 L, respectively. From day 181 to the end of the year all configurations follow a smooth increasing line up to an availability of 0.90 for no hot water storage, 0.96 for 1000 L and 0.97 for a 5000 L hot water storage. The availability of the cogeneration system is mainly affected by the existence of a hot water reservoir and to a lesser extent by its size. For example, towards day 365, the availability with no hot water storage is

approximately 0.90, a value that increases by 6% when a 1000 L storage is added, but increases by 7% when the volume of hot water storage increases to 5000 L.

A different situation can be observed when a triangular hot water consumption profile is considered (Figure 6b). From the beginning of the year, the relative importance of the additional hot water volume above 2000 L is not very clear before day 150. This behavior allows to deduce that the buffer effect of the storage makes it possible to decouple the heat generation from the consumption by reducing the cycling of diesel boiler. Consequently, the result is better operating behavior and higher fuel consumption efficiency. In the absence of hot water storage, the system starts with a value around 0.71 during first month and then shows an increase in availability due to the decrease in hot water consumption in March and April. While in the following months of May, June and July there is a decrease in availability due to an increase of hot water demand.

Before day 150, *i.e.*, when the hot water demand is relatively low due to the summer season, configurations using storage volumes of 2000, 3000, 4000 and 5000 L almost reach the maximum availability with small differences between them. After day 150, there is a sharp increase in the hot water consumption which leads to a significant reduction in availability, regardless of the configuration analyzed. However, larger volumes of hot water reservoirs exhibit small slopes, resulting in a reduced effect of heat demand on the availability.

Figure 6c shows the daily evolution of system availability over the year for the hot water consumption profile 3. This profile is based on domestic hot water consumption according to ISO 9459-3:1007 [28] and is widely used for residential applications. The first point to observe is the important role that hot water storage tanks plays on the availability of the system, indeed larger volumes increase availability along the year. In general, the availability dynamics are similar for system with a storage volume of 2000, 3000, 4000 and 5000 L. Moreover, when no hot water storage is used, the availability index converges rapidly at the beginning of the year. The addition of a 1000 L reservoir improves availability by an average of about 10%. The situation is different when the size of the reservoir increases beyond 1000 L because there is an important increase in availability between day 30 and 120. This makes it possible to better cope with the increase of heat consumption in winter.

This increasing gap in availability between two storage size appears to be reduced as the volume increases, thus reducing the buffering effect. Maximum variations are found on day 120, with availability values of 0.66 for no reservoir and 0.68, 0.79 and 0.88 for reservoir of 1000, 3000 and 5000 L, respectively.

Figure 6d shows the daily availability of the cogeneration system over the year for profile 4. As in the previous case, since heat consumption is concentrated over a limited range around midday, there is no volume studied that allows decoupling heat production from consumption. Moreover, the additional gain in system availability decreases asymptotically as the volume increases. The system availability with no hot water reservoir is almost constant over the year with a minimum of 0.625 and a maximum of 0.635. When a 1000 L hot water reservoir is included, availability increases from 0.7083 at its minimum and to 0.77 at its maximum. Better results are obtained when the reservoir size is further increased to 3000 L. However, when size increases to 5000 L, the effect on availability is not as significant as the increase from 1000 to 3000 L, possibly because the system is approaching its maximum. For example, the variation on day 150 (when an important increase in monthly hot water demand is reported) is around 20% when going from no reservoir to a 1000 L reservoir, then 23% when increasing size from 1000 to 3000 L, but only 4.1% when going from 3000 to 5000 L.

Figure 6e shows the availability results for profile 5, which corresponds to a cascade consumption from 7 to 15 h. In general, the results for this profile are more stable. The dynamic behavior of system availability for the six configurations studied follows same trend. From the beginning of the period, all the configuration systems evolve by increasing the availability until a maximum that is found at day 120, which corresponds to the moment when the hot water consumption increases considerably due to the winter season, thus reducing the buffer capacity of systems. After day 120, all systems reduce their availability smoothly to a minimum that is reached around day 243, when the daily hot water consumption is about 21.370 L/day. It can be observed that along the year, the buffer effect is reduced when the volume of the buffer tank increases. For example, on the day of maximum availability (day 120) the additional gain from adding a 1000 L reservoir is 8%, from 1000 to 2000 L is 3.7%, then from 2000 to 3000 L is 2.47% to reach

a minimum of 1.18% when the volume increases from 3000 to 4000 L. Nevertheless, when the storage volume increases from 4000 to 5000 L, the gain becomes more important again.

Finally, Figure 6f shows the daily evolution of the cogeneration system availability for the hot water consumption profile 6. In this profile, consumption is concentrated between 13 to 15 h with 90% of total daily consumption, with the other 10% consumed at 16 h. The results show that any storage volume studied can make a buffer effect to be coupled with the heat demand. If the case of no heat storage is considered, the availability is around 0.795 over the year. When a 1000 L storage volume is added, availability increases to 0.833, improving availability by about 4.77%, but when the volume increases to 2000 L, no contribution to availability can be observed. A slight improvement in availability is observed between 2000 and 3000 L, which means that the concentration of hot water consumption in the afternoon prompts the system to have more storage volume, thus reducing boiler operation. However, when a reservoir of 5000 L is included, the availability increases to 87.5% from the beginning of the year to day 150, when it begins to drop smoothly to 85.95% on day 250. From day 250 until the end of the year, the availability increases slightly to 86.79%. When heat consumption is concentrated over a part of the day, the size of the volumes studied is not sufficient to obtain a maximum buffering effect due to the large amount of water consumed in such a short time. For this case, system availability can still be improved by increasing the size of the hot water reservoir.

4.2. Annual average

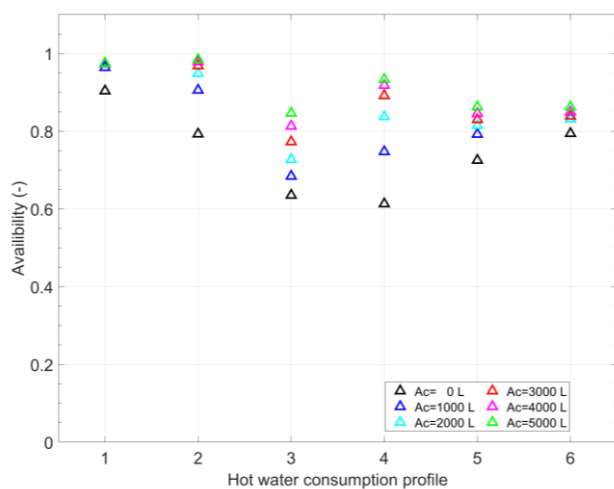


Figure 7. Cogeneration system availability as a function of hot water demand profile for the four water storage sizes.

The annual average for availability, operational cost and CO_2 emissions of the cogeneration system is evaluated in the following.

Figure 7 shows the annual availability for the different combinations of hot water storage configuration and hot water consumption profile. This allows us to quantify the annual effect of different hot water storage sizes for each hot water consumption profile. As expected, when the amount of stored hot water increases, the availability of the cogeneration system also increases, since the hot water reservoir has a buffering effect on the system, reducing thus the impact of variability in the demand. In general, the buffer inventory level should provide the proper isolation time before the buffer becomes empty, so that during this time a maintenance intervention or a demand change can be carried without causing a propagation of the effect of the failure or of the demand variability in the machines downward [24]. Therefore, regardless of the hot water consumption profile, the best availability is obtained by using the 5000 L storage volume; however, the availability in the other storage configurations varies according to the hot water consumption profile. The results clearly show that for hot water consumption profile 1, the availability of the cogeneration system improves with a hot water storage but is almost not affected by its size. In contrast, profile 2 is more sensitive than profile 1 to the addition of a hot water storage and its size, but the difference between the availability values decreases with increasing hot water storage size. Availability for the hot water profile 3 has a linear effect with the addition of a hot water storage, as its availability increases from 0.63 with no storage up to 0.84 with a hot water storage volume of 5000 L. The availability of the system with profile 4 is also affected according to the hot water storage configuration, which translates into an increase from 0.61 with no hot water storage, to 0.74, 0.83, 0.89, 0.91 and 0.93 for hot water storage volumes of 1000, 2000, 3000, 4000 and 5000 L, respectively. For profile 5, the addition of a 1000 L hot water storage increases the availability by about from 0.72 to 0.79. Afterwards, the addition of larger hot water storage volumes is by far less sensitive to the availability index for this profile. Finally, the average annual availability of hot water consumption profile 6 is remarkably affected only when a 1000 L hot water storage is included. This means that there is a minimum amount of stored hot water

needed to increase availability, which should be considered when designing a system for similar hot water consumption profiles.

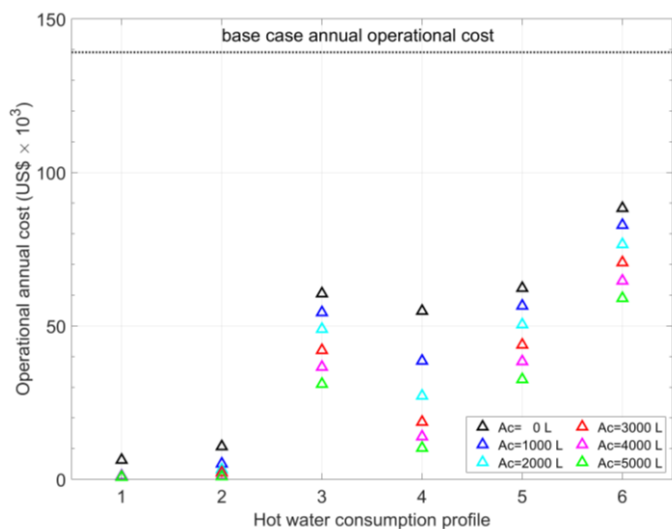


Figure 8. Operational annual cost of the cogeneration system as a function of hot water demand profile for the six water storage sizes.

Table 8. Statistics of availability for different profiles.

Profile	Mean	Std	Min	Max
1	0.96	0.03	0.90	0.98
2	0.93	0.07	0.79	0.98
3	0.75	0.08	0.64	0.85
4	0.82	0.12	0.61	0.93
5	0.81	0.05	0.73	0.86
6	0.83	0.02	0.79	0.86

Table 8 data reveals variations in the availability of the cogeneration system across different profiles. Profiles 1 and 2 demonstrate relatively higher mean availability, indicating more reliable performance. Profiles 3, 4, and 5 exhibit lower mean availability, suggesting a less dependable operation. Profile 6 stands out with a slightly higher mean availability compared to the previous profiles. The standard deviations provide insights into the variability of availability within each profile. These statistics can serve as valuable inputs for reliability and availability modeling in the research paper, enabling a comprehensive analysis of the system's performance in meeting the heat and hot water demands of the isolated Antarctic base.

The cogeneration system reduces operational annual costs because of the savings in diesel fuel consumed by the conventional boiler currently used to satisfy the hot water demand of the base.

The operational annual cost of each evaluated case (**Błąd! Nie można odnaleźć źródła odwołania.**) is calculated considering the installation and fuel costs used in the boiler. The use of the heat recovery system is largely justified with any of hot water consumption profile and hot water storage configuration systems. The lowest annual costs are obtained for uniformly and triangular distributed daily consumption profiles (profile 1 and 2), with similar total annual costs. Also, for these two profiles, the annual costs are less sensitive to the hot water storage configuration than the rest of the consumption profiles. Profile 3 is the most sensitive to the hot water storage configuration, with an operational annual cost between 61 and 31k USD, whereas for profiles 4 and 5, the cost varies from 54 to 10k and 62 to 32k USD, respectively. Profiles 4 and 5 are quite similar despite the noticeable differences in system availability under the same conditions, highlighting the importance of considering cost along with availability. Total operational annual cost for profile 6 is higher than for the other profiles regardless of hot water storage configuration (59-88 k USD), but the distribution of costs between the different volumes is quite similar to those of profiles 4 and 5.

Table 9. Statistics of operation cost (US\$ x 10³) for different profiles.

Profile	Mean	Std	Min	Max
1	1.77	2.22	0.72	6.29
2	3.88	3.65	0.94	10.68
3	45.58	11.10	31.04	60.51
4	27.23	16.92	10.19	54.83
5	47.32	11.21	32.55	62.28
6	73.67	11.06	59.00	88.32

Table 9 provides information about the six hot water consumption profiles and their corresponding mean, standard deviation, minimum, and maximum operation costs in thousands of US dollars. Data reveals considerable variations in the operation costs for different hot water consumption profiles. Profiles 3, 5, and 6 stand out with significantly higher mean costs compared to the rest, suggesting a greater demand for more intensive hot water usage. The standard deviations provide insights into the variability of costs within each profile. These statistics can serve as valuable inputs for reliability and availability modeling in the research paper, allowing for a comprehensive analysis of the cogeneration system's

performance and associated costs in meeting the heat and hot water demands of the isolated Antarctic base.

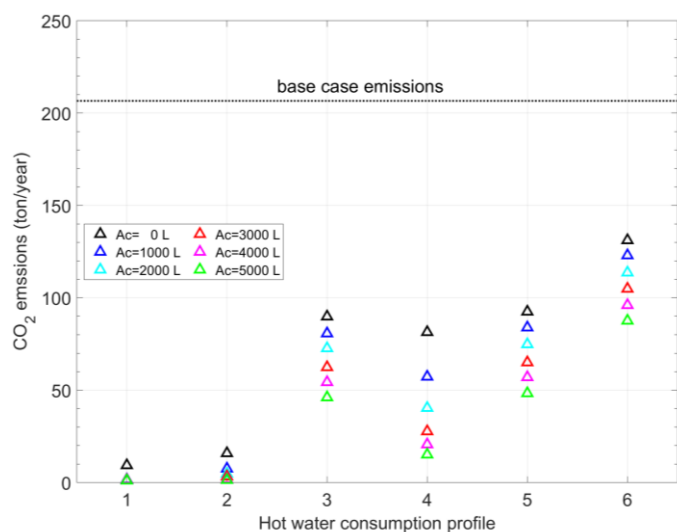


Figure 9. Cogeneration system emissions as a function of hot water demand profile for the four water storage sizes.

Finally, the environmental impact of implementing a waste heat recovery system in a diesel generator system is estimated. The potential reduction in emissions from the cogeneration system is calculated based on the displacement of boiler fossil fuel consumption, which reduces CO_2 and other GHG emissions into the atmosphere, contributing to the reduction of global warming. **Błąd! Nie można odnaleźć źródła odwołania.** compares the emissions of the 36 simulated system configurations with the emissions of the base case, where no waste heat recovery is considered, and hot water is supplied only with an oil boiler.

As expected, the results follow the same trend as cost. From an environmental point of view, the inclusion of a waste heat recovery system significantly reduces emissions regardless of storage configuration or hot water consumption profile. On average, the lowest emissions occur for profile 1 with reservoir, where almost all water needed for the base is supplied by the cogeneration system.

In the other side, highest emissions are produced for profile 6 without hot water reservoir. Another important thing is that the effect of hot water storage size on CO_2 emissions is quite similar for profiles 3 and 5, which results in a reduction variation of around -11% when comparing no reservoir and a 1000 L reservoir, -22% when comparing 1000 and 3000 L reservoirs, and -26% when comparing 3000 and 5000 L

reservoirs. The sensitivity of CO_2 emissions according to profile 4 is remarkably more important than the rest of profile, with a range between 81 and 15 ton/year of CO_2 emissions for no hot water reservoir and a 5000 L reservoir, whereas for profiles 1 and 2 this range is 10-1 and 16-1.4 CO_2 ton/year, respectively.

Table 10 provides statistics of CO_2 emissions (ton/year) for different hot water consumption profiles. The data reveals significant variations in CO_2 emissions associated with different hot water consumption profiles. Profiles 3, 5, and 6 stand out with considerably higher mean emissions compared to the other profiles, indicating a greater environmental impact. Profiles 1 and 2 show relatively lower mean emissions. The standard deviations provide insights into the variability of emissions within each profile. These statistics can serve as valuable inputs for analyzing and comparing the environmental sustainability of the hot water consumption profiles in the research paper.

Table 10. Statistics of CO_2 emissions (ton/year) for different hot water consumption profiles.

Profile	Mean	Std	Min	Max
1	2.63	3.29	1.07	9.34
2	5.76	5.42	1.39	15.87
3	67.68	16.48	46.09	89.85
4	40.43	25.13	15.14	81.41
5	70.27	16.65	48.33	92.48
6	109.38	16.43	87.60	131.15

5. Conclusions

The impacts of hot water consumption profile and hot water reservoir volume on the cogeneration system are presented and discussed in this paper. The cogeneration system delivers electricity and thermal energy to water for space and domestic hot water heating purposes. The study was conducted using the operational diesel fuel consumption of an Antarctic Chilean base. A model based on energy balances was used to estimate heat recovered from exhaust gases. The reliability of the cogeneration system is modelled based on state space and on a continuous Markov process by applying a frequency-balance method.

The results of assessing reliability and availability of heat recovery system showed that increasing the volume of hot water reservoir increased the availability of the cogeneration system because of the buffer effect. It is interesting to note that this effect is not linear, and it depends on the hot water consumption

profile and thus, when sizing this kind of systems, both, hot water reservoir volume and hot water consumption profile should be considered. The availabilities, found for the different cases evaluated, were used to obtain annual operational costs and annual emissions. If the hot water consumption profile is not uniform along the day, it is very difficult for the system to decouple heat production from consumption for the storage volumes studied. Hot water profiles 1 and 2, corresponding to

uniform and triangular distributions over the day, respectively, exhibited similar annual operational costs regardless the hot water reservoir volume.

Thus, the reliability and availability modelling, along with the sensitivity analysis, of CHP components presented here can be useful in feasibility studies of retrofitted waste heat recovery systems and in determining their optimal design and operational parameters.

Nomenclature

Greek Symbols		Roman Symbols	
α	Correlation parameter	A	Availability
β	Correlation parameter	AC	Annual operational cost (USD)
λ	Failure rate	c_p	Specific heat (kJ/kg K)
μ	Repair rate	CCHP	Combined cooling, heating, and power
η	Efficiency	\dot{E}	Energy rate supply (kW)
ρ	Density (kg/l)	de	Electric demand (kW)
ϕ	Fraction of energy lost through exhaust gases	F	Demand factor
Subscripts		CHP	Combined heat and power
b	Boiler	dt	Hot water demand profile (L) generated
chp	CHP system	GHG	Greenhouse gases
cws	Cold water system	LHV	Lower calorific value of the fuel (kJ/kg)
e	Electric system	\dot{m}	mass flow (kg/s)
exh	exhaust gases	\dot{Q}	Energy (kW)
f	Fuel system	P	Probability
h	Heat recovery	R	Reliability
hrs	Hot water system	RES	Renewable energy sources
r	Recovery system	S	Subsystem
s	System	T_i	Initial temperature (K)
w	Water	T_0	Final temperature (K)

References

1. Araya R, Bustos F, Contreras J, Fuentes A. Life-cycle savings for a flat-plate solar water collector plant in Chile. *Renewable Energy*. 2017; 112:365–77. doi:10.1016/j.renene.2017.05.036.
2. Asaee SR, Ugursal VI, Beausoleil-Morrison I. An investigation of the techno-economic impact of internal combustion engine based cogeneration systems on the energy requirements and greenhouse gas emissions of the Canadian housing stock. *Applied Thermal Engineering*. 2015; 87:505–18. doi:10.1016/j.applthermaleng.2015.05.031.
3. Asaee SR, Ugursal VI, Beausoleil-Morrison I. Techno-economic evaluation of internal combustion engine based cogeneration system retrofits in Canadian houses – A preliminary study. *Applied Energy*. 2015; 140:171–83. doi:10.1016/j.apenergy.2014.11.068.
4. Azarkish H, Rashki M. Reliability and reliability-based sensitivity analysis of shell and tube heat exchangers using Monte Carlo Simulation. *Applied Thermal Engineering*. 2019;159:113842. doi:10.1016/j.applthermaleng.2019.113842.
5. Billinton R, Allan RN. Reliability evaluation of engineering systems: Concepts and Techniques. New York: Springer; 1992. doi:10.1007/978-1-4899-0685-4.

6. Cai B, Li H, Hu Y, Zhang G. Operation strategy and suitability analysis of CHP system with heat recovery. *Energy and Buildings*. 2017; 141:284–94. doi:10.1016/j.enbuild.2017.02.056.
7. Conklin JC, Szybist JP. A highly efficient six-stroke internal combustion engine cycle with water injection for in-cylinder exhaust heat recovery. *Energy*. 2010; 35(4):1658–64. doi:10.1016/j.energy.2009.12.012.
8. Deelaman W, Pongpiachan S, Tipmanee D, Suttinun O, Choochuay C, Iadtem N, Charoenkalunyuta T, Promdee K. Source apportionment of polycyclic aromatic hydrocarbons in the terrestrial soils of King George Island, Antarctica. *Journal of South American Earth Sciences*. 2020; 104:102832. doi:10.1016/j.jsames.2020.102832.
9. Dincer I, Rosen MA. Chapter 12 - Exergy analysis of cogeneration and district energy systems. In: Dincer I, Rosen MA, editors. *Exergy*. Amsterdam: Elsevier; 2007. p. 257–76. doi:10.1016/B978-008044529-8.50015-X.
10. Farhat O, Faraj J, Hachem F, Castelain C, Khaled M. A recent review on waste heat recovery methodologies and applications: Comprehensive review, critical analysis and potential recommendations. *Cleaner Engineering and Technology*. 2022; 6:100387. doi:10.1016/j.clet.2021.100387.
11. Gang W, Wang S, Xiao F, Gao D ce. Robust optimal design of building cooling systems considering cooling load uncertainty and equipment reliability. *Applied Energy*. 2015; 159:265–75. doi:10.1016/j.apenergy.2015.08.070.
12. Ge Z, Zhang Y, Wang F, Luo X, Yang Y. Virtual–real fusion maintainability verification based on adaptive weighting and truncated spot method. *Eksplloatacja i Niezawodność – Maintenance and Reliability*. 2022;24(4):738-746. <https://doi.org/10.17531/ein.2022.4.14>
13. Georgilakis PS, Katsigiannis YA. Reliability and economic evaluation of small autonomous power systems containing only renewable energy sources. *Renewable Energy*. 2009;34(1):65–70. doi:10.1016/j.renene.2008.03.004.
14. Haghifam MR, Manbachi M. Reliability and availability modelling of combined heat and power (CHP) systems. *International Journal of Electrical Power & Energy Systems*. 2011;33(3):385–93. doi:10.1016/j.ijepes.2010.08.035.
15. Hatami M, Ganji DD, Gorji-Bandpy M. A review of different heat exchangers designs for increasing the diesel exhaust waste heat recovery. *Renewable and Sustainable Energy Reviews*. 2014; 37:168–81. doi:10.1016/j.rser.2014.05.004.
16. Hoang AT. Waste heat recovery from diesel engines based on Organic Rankine Cycle. *Applied Energy*. 2018; 231:138–66. doi:10.1016/j.apenergy.2018.09.022.
17. Jiang J, Wei X, Gao W, Kuroki S, Liu Z. Reliability and Maintenance Prioritization Analysis of Combined Cooling, Heating and Power Systems. *Energies*. 2018;11(6). doi:10.3390/en11061519.
18. Jiang J, Gao W, Wei X, Li Y, Kuroki S. Reliability and cost analysis of the redundant design of a combined cooling, heating and power (CCHP) system. *Energy Conversion and Management*. 2019; 199:111988. doi:10.1016/j.enconman.2019.111988.
19. Karki R, Billinton R. Cost-effective wind energy utilization for reliable power supply. *IEEE Transactions on Energy Conversion*. 2004 Jun;19(2):435–40. doi:10.1109/TEC.2003.822293.
20. Kozłowski E, Borucka A, Świdorski A. Application of the logistic regression for determining transition probability matrix of operating states in the transport systems. *Eksplloatacja i Niezawodność – Maintenance and Reliability*. 2020;22(2):192-200. <http://dx.doi.org/10.17531/ein.2020.2.2>.
21. Kristjanpoller F, Crespo A, Barberá L, Viveros P. Biomethanation plant assessment based on reliability impact on operational effectiveness. *Renewable Energy*. 2017; 101:301–10. doi:10.1016/j.renene.2016.08.065.
22. Kristjanpoller F, Viveros P, Zio E, Pascual R, Aranda O. Equivalent availability index for the performance measurement of haul truck fleets. *Eksplloatacja i Niezawodność*. 2020;22(4):583–91. doi:10.17531/ein.2020.4.1.
23. Lingeswara S, Omar R, Ghazi TIM. Reliability analysis on a shell and tube heat exchanger. *IOP Conference Series: Earth and Environmental Science*. 2016 Jun;36(1):012012. doi:10.1088/1755-1315/36/1/012012.
24. Luján JM, Climent H, Dolz V, Moratal A, Borges-Alejo J, Soukeur Z. Potential of exhaust heat recovery for intake charge heating in a diesel engine transient operation at cold conditions. *Applied Thermal Engineering*. 2016; 105:501–8. doi:10.1016/j.applthermaleng.2016.03.028.
25. Macchi M, Kristjanpoller F, Garetti M, Arata A, Fumagalli L. Introducing buffer inventories in the RBD analysis of process production systems. *Reliability Engineering & System Safety*. 2012; 104:84–95. doi:10.1016/j.res.2012.03.015.
26. Oszczypała M, Ziółkowski J, Małachowski J. Semi-Markov approach for reliability modelling of light utility vehicles. *Eksplloatacja i*

Niezawodność – Maintenance and Reliability. 2023;1 25(2). <https://doi.org/10.17531/ein/161859>.

27. Pandiyarajan V, Pandian MC, Malan E, Velraj R, Seeniraj RV. Experimental investigation on heat recovery from diesel engine exhaust using finned shell and tube heat exchanger and thermal storage system. *Applied Energy*. 2011;88(1):77–87. doi:10.1016/j.apenergy.2010.07.023.
28. Performance test for solar plus Supplementary Systems [Internet]. Vol. 1997. Geneva, CH: International Organization for Standardization; 1997 Mar. Available from: <https://www.iso.org/standard/20488.html>.
29. Rodríguez LR, Lissén JMS, Ramos JS, Jara EÁR, Domínguez SÁ. Analysis of the economic feasibility and reduction of a building's energy consumption and emissions when integrating hybrid solar thermal/PV/micro-CHP systems. *Applied Energy*. 2016; 165:828–38. doi:10.1016/j.apenergy.2015.12.080.
30. Rusin A, Tomala M. Steam turbine maintenance planning based on forecasting of life consumption processes and risk analysis. *Eksplatacja i Niezawodność – Maintenance and Reliability*. 2022;24(3):1. <https://doi.org/10.17531/ein.2022.3.1>.